Collapse Analysis of Spot Welded Thin Section Members in a Vehicle Body Structure at Various Impact Velocities

Cheon Seok Cha, Jae Oh Chung
Division of Mechanical and Automotive Engineering, Sunchon National University, Suncheon, Jeonnam 540-742, Korea
Jae Woung Park
Division of Aerospace and Naval Architectural Engineering, Chosun University, Kwang-ju 501-759, Korea
Young Nam Kim, In Young Yang*
Division of Mechanical Engineering, Chosun University, Kwang-ju 501-759, Korea

The spot welded sections of automobiles such as the hat and double hat section members, absorb the most of the energy during the front-end collision. The purpose of this study was to analyze the collapse characteristics of spot welded section members with respect to the pitch of spot welds on flanges, through impact experiments and computation for para-closed sections and perfectly closed sections. The hat shaped section members were tested at the impact collapse velocities of 4.72 m/sec, 6.54 m/sec and 7.19 m/sec and double hat shaped section members were tested at the impact collapse velocities of 6.54 m/sec, 7.19 m/sec and 7.27 m/sec. A commercial LS-DYNA3D was used to simulate the collapse behavior of the hat and double hat shaped section members. The validity of the simulation was to be proved by comparing the simulation results and the experimental results.

Key Words : Spot Welded Sections of Automobiles, Front-end Collision, Spot Welded Pitch, Impact Collapse Velocities, Collapse Characteristics

1. Introduction

Autombiles are designe mainly is to satisfy the standards and the requirements of general performance, stability, calmness and firm handling. The ability to protect passengers on a car accident depends on the conditions of the collision, structural integrity and passenger protective equipment. Since it is a most frequent one, attention to safety has increasingly been paid on the front-end collisions (John Fenton, 1996 ; Haug et al., 1996 ; Hanssen et al., 1999).

* Corresponding Author.
E-mail : iyyang@mail.chosun.ac.kr
TEL : +82-62-230-7170; **FAX** : +82-62-230-7170
Division of Mechanical and Automotive Engineering, Sunchon National University, Suncheon, Jeonnam 540-742, Korea. (Manuscript **Received** May 6, 2002; **Revised** September 3, 2002)

Notably, section members of the front-head absorb most of the energy on the front-end collision (Singace, 1999 ; Avalle et al., 1997). Many vehicles have been designed to absorb the front-end collision impact energy through plastic deformation of hat shaped section members. Thus it is of importance that we understand the characteristics of energy absorption and the collapse behavior of plastic deformation on a simple structure, which endures a massive collision (White et al., 1999a ; White et al., 1999b ; Cha et al., 2001 ; Grzebieta et al., 1986 ; Jonse, 1989).

In this study, we analyzed the collapse characteristics of spot welded hat and double hat shaped section members under the impact collapse, at various spot welded pitches. In particular, the spot welded hat shaped section members were not perfectly closed sections but para-closed sections. Impact collapse experiments were performed with

respect to the various impact velocities, because it was thought that para-closed sections would show collapse characteristics quite different from those of perfectly closed sections. In this study, an explicit finite element code, LS-DYNA3D, and impact collapse experiments were used for the analysis.

2. Specimens and Impact Collapse Experiment

The specimens, of hat and double hat shaped section members, were manufactured by welding two parts as shown in Fig. 1 using SCP1 cold rolled steel sheet. Section members of 0.78 mm thickness, 30×30 mm width ratio, and 12 mm width flange were prepared. Three types of spot welded pitch for tests were 18.3 mm, 22 mm and 27.5 mm. Table 1 shows the material constants of specimens and Table 2 describes the specimens.

Table 1 Material constants of specimens

Yield strength [MPa]	Tensile strength [MPa]	Young's modulus [GPa]	Poisson's ratio	Elongation [%]
166.7	308.4	203	0.31	46.4

Table 2 Definition of specimens

H(D) E(F, G) In

Type
- H : Hat shaped
- D : Double hat shaped

Spot weld pitch
- E : 18.3 mm
- F : 22.0 mm
- G : 27.5 mm

Impact Velocities
- n=0 : 4.72 m/sec
- n=1 : 6.54 m/sec
- n=2 : 7.19 m/sec
- n=3 : 7.27 m/sec

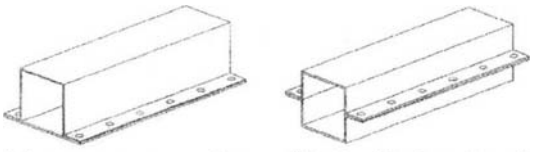

(a) Hat shaped section member (b) Double hat shaped section member

Fig. 1 Configuration of the specimens

The axial impact collapse test device, which used compressed air is presented in Fig. 2, and a system diagram is shown Fig. 3. In the impact collapse test, the cross head is pressured by the

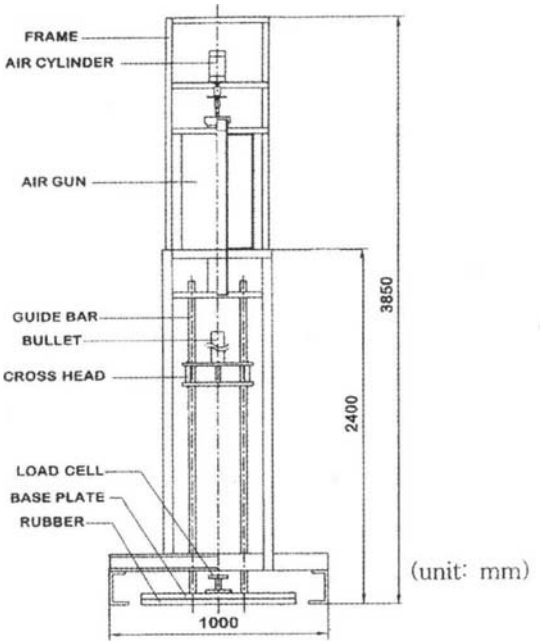

Fig. 2 Impact testing setup for crushing

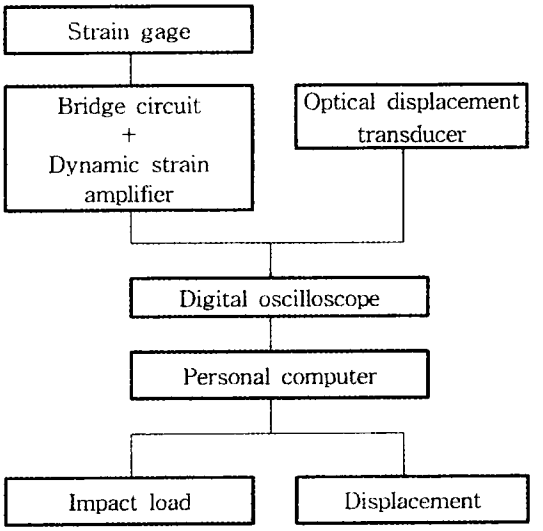

Fig. 3 Diagram of measurement system

axial impact collapse test device using an air pressure accelerator (Cha et al., 2001).

After an axial collapse test, the load and deformation of the collapse course were measured. A load-displacement curve for the collapse history was obtained by eliminating the time axis from the measured time-load and time-displacement curves. The absorbed energy is equal to the area below the load-displacement curves, and is calculated by integrating the load with respect to the displacement as Eq. (1). The mean collapse load (P_{mean}) is obtained by dividing the absorbed energy (E_a) by the displacement.

$$E_a=\int_{l_0}^{l} Pdl$$
$$P_{mean}=\frac{E_a}{l-l_0} \tag{1}$$

where E_a is the absorbed energy in the specimen and P is the collapse load.

Based on the load-displacement curve, total absorbed energy (E_L), maximum collapse load ($P_{max.}$) and deformed length (S) were derived. The absorption characteristics of each specimen was studied. The specimens did not collapse equally in length, though the cross head imposed the same impact energy under the same condition. It was assumed that specimens would collapse as much as the total length of 120 mm in order to analyze the total absorbed energy quantitatively. The total absorbed energy (E_L) is given as below Eq. (2).

$$E_L=E_a\bar{J} \tag{2}$$

where $\bar{J}(=L/S)$ is the inverse stroke efficiency, S is the deformed length and L is the total length before deformation.

The value of the impact energy (E_I) is similar to that given by Eq. (3): 446 J at 4.72 m/sec, 855 J at 6.54 m/sec, 1034 J at 7.19 m/sec and 1057 J at 7.27 m/sec.

$$E_I=\frac{1}{2}mv^2 \tag{3}$$

where m is the mass of the cross head (40 kilograms) and v is the impact collapse velocity.

The impact collapse velocities were selected as follows: the velocities in the hat shaped section members were 4.72 m/sec, 6.54 m/sec and 7.19 m/sec and those in the double hat shaped section members were 6.54 m/sec, 7.19 m/sec and 7.27 m/sec. The velocities were selected due to the energy absorption capability of section members during the impact collapse. The higher velocity could not be selected owing to the limits of energy absorption ability of section members.

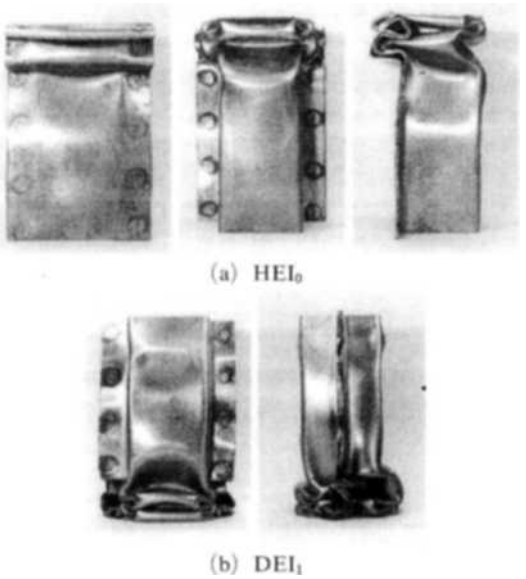

Fig. 4 Shape of collapsed specimens

Figure 4 represents the shape of collapsed specimens of hat and double hat shaped section members with a spot welded flange pitch of 18.3 mm. Figure 4(a) is a shape of the collapsed hat shaped section members after a free drop velocity impact of 4.72 m/sec. Figure 4(b) represents the shape of collapsed specimens after the impact experiment was conducted at the impact velocity (6.54 m/sec, impact energy 855 J), under the air pressure of 0.3 MPa in the double hat shaped section members.

3. Impact Collapse Simulation

In the program system presented in this study, an explicit finite element code, LS-DYNA3D (Livermore Software Technology, 1997), was adopted to simulate the complicated collapsed behavior of the hat and double hat shaped section

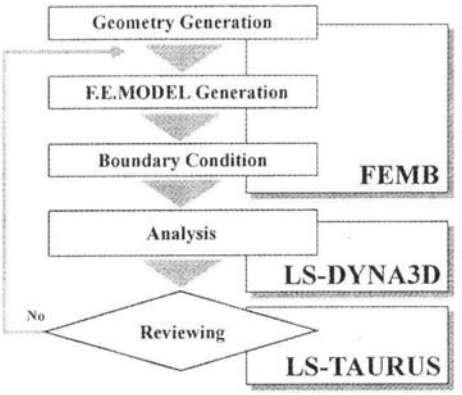

Fig. 5 Procedure of dynamic axial collapse analysis

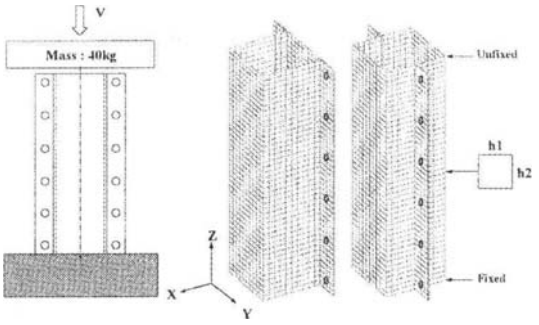

Fig. 6 Boundary condition of impact collapse

members.

The simulation does not only estimate the efficiency under various condition by using an assumed FEM model, but also reduces the developing period by pre-estimating the effect of structural change in advance. By using FEM, it is possible to pre-estimate the effect of interference or shape from impact phenomenon in very short time, and to obtain the complex distribution of stress-deformation which cannot be estimated by experiment. The purpose of analyzing the impact mechanism is to understand the impact characteristics of section members, to obtain the valid information and to utilize it in the optimum car structure design.

Figure 5 shows the history of carrying out the impact collapse simulation, and Figure 6 represents the finite element model used in the impact collapse simulation, with its boundary conditions.

The dimensions of the model are the same as

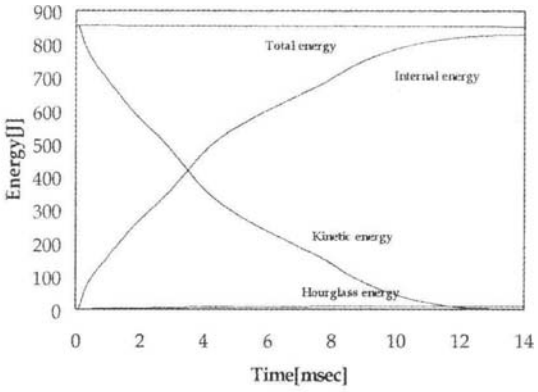

Fig. 7 Relationship between time and energy, DEI_1

those of the experiments. The hat and double hat shaped section members are divided into Belytschko-tsay shell elements (Livermore Software Technology, 1993), with four nodal shell elements of h1 (3 mm) × h2 (3 mm).

Considered the conditions of the experiment, it was assumed that the bottom of the model be fully restrained and the top of the model remain free. An arbitrary finite stone wall of mass of 40 kg is placed at a certain distance from the top, and strikes the top of the model at a velocity V. The impact velocity of the simulation is the same as that used in the actual experiment.

The stone wall is defined as a master that strikes a slave, the nodes on the top of the specimen. Because the distinction of the analytical result according to contact is very small and because the contact problem is out of the interest after the occurrence of the first folding mode, an AUTOMATIC SINGLE SURFACE was selected.

The hourglass energy has been controlled to make out how it affects the total absorbed energy. As shown in Fig. 7, the hourglass energy is less than ane percent of the total energy. This may imply that the analysis is reliable.

The material properties used in simulation are the material constants, which were obtained by tensile testing. All shells in the model were adapted to conform with the stress-deformation relationship in order to consider the linear and non-linear behaviors. Because of the strain rate sensitivity, the maximum collapse loads from tests

are higher than the yield point load. Therefore, the simulation considered the strain rate sensitivity. In the process, the Eq. (4) of Couper Symonds was considered.

$$\sigma_n=\sigma_y\left(1+\left(\frac{\dot{\varepsilon}}{D}\right)^{1/q}\right) \qquad (4)$$
$$\dot{\varepsilon}=\sqrt{\dot{\varepsilon}_{ij}\dot{\varepsilon}_{ij}}$$

where σ_y is the static yield stress, σ_n is the yield stress in high speed deformation, $\dot{\varepsilon}$ is the strain rate, $\dot{\varepsilon}_{ij}$ is the strain rate tensor, i and j have the range 1 to 3, when 1, 2 and 3 are identified with the cartesian coordinates x, y and z, respectively. D and q are strain rate parameters. In this study, $D=40.4\ s^{-1}$ and $q=5$ were applied by doing high speed tensile tests on SCP1 cold rolled steel (Grxebieta et al., 1986 ; Jones, 1989).

In order to get the same collapse mode as in the experiment, center nodes on the top of the double hat shaped section member were moved by 0.03%. However, the imperfections on the hat shaped section members were not applied because its collapse mode was decided by the buckling of the plane which is lower than that of the open square channel section.

Figure 8 shows the history of collapse after simulating a section member with a spot welded flange pitch of 18.3 mm. Figure 8(a) shows the history of collapse of the hat shaped section member under the impact collapse velocity of 4.72 m/sec (impact energy 446 J), and Fig. 8(b) shows the history of collapse of the double hat shaped section member under the impact collapse velocity of 6.54 m/sec (impact energy 855 J).

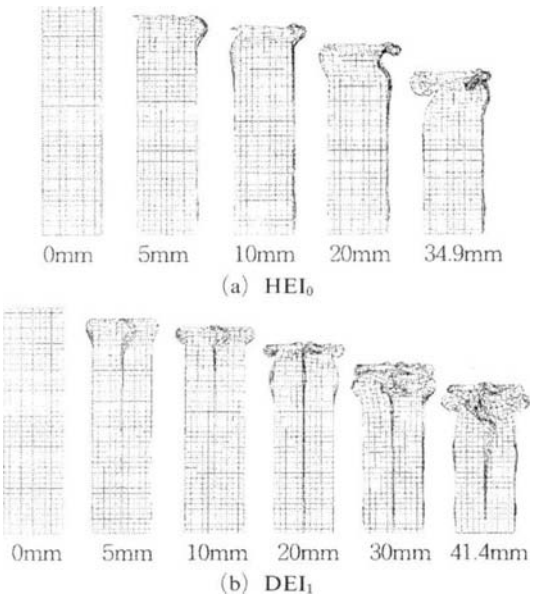

Fig. 8 Collapsing process of specimens

4. Results and Discussion

In Table 3, the absorbed energy, total absorbed energy, mean collapse load, maximum collapse load and deformed length in the experiment and simulation are compared with respect to various section dimensions.

In Figs. 11 and 12, the mean collapse loads in the experiment and simulation are compared with respect to the variations of the spot welded pitch on the flanges at the velocity of 6.54 m/sec and 7.19 m/sec. In Figs. 13, 14 and 15, the mean collapse loads in the experiment and simulation are compared at various velocities (impact energies) for spot welded pitches of 18.3 mm, 22 mm and 27.5 mm.

In Table 3, Figs. 11 and 12, in the hat and double hat shaped section members at the respective velocities, the larger the flange welded pitch is, the lower the mean collapse load in the experiment and simulation is. This is the reason why the mean collapse load drops owing to the size of welded pitch becoming larger. The size of the first folding length appears to depend upon the welded pitch. Figure 9 shows the first folding length in the hat shaped section members under collapse, and in Fig. 9(a) l_0 expresses the size of l_E, l_G in Fig. 9(b). l_E is the first folding length at the welded pitch (18.3 mm), l_G is the first folding length when the welded pitch in the hat shaped section member is 27.5 mm. Figure 10 shows a compares the first folding lengths in double hat shaped section members of welded pitch 18.3 mm and 27.5 mm. As shown in the figure, section members whose welded pitch is short, show that the total absorbed energy and mean collapse loads are high, because the first folding length is so short that its strength is much higher than the section members whose welded pitch is longer.

Table 3 Collapse test and simulation results for hat and double hat shaped section members at different flange spot-weld pitches and impact velocities

Spec.	Absorbed energy, E_a[J]		Total absorbed energy E_L[J]			Mean collapse load P_{mean}[kN]			Maximum collapse load, $P_{max.}$ [kN]			Deformation S[mm]	
	test $(E_a)t$	simulation $(E_a)s$	test $(E_L)t$	simulation $(E_L)s$	sim./ test	test $(P_{mean})t$	simulation $(P_{mean})s$	sim./ test	test $(P_{max.})t$	simulation $(P_{max.})s$	sim./ test	test $(S)t$	simulation $(S)s$
HEI_0	438.5	435.0	1315.5	1495.7	1.137	11.0	12.5	1.136	59.3	64.6	1.089	40	34.9
HFI_0	434.5	432.6	1212.4	1380.6	1.139	10.1	11.5	1.139	60.2	65.4	1.087	43	37.6
HGI_0	424.1	433.3	1156.6	1296.7	1.121	9.6	10.8	1.125	58.6	63.6	1.085	44	40.1
HEI_1	826.2	832.5	1458.0	1637.7	1.123	12.2	13.7	1.123	61.0	69.7	1.143	68	61.0
HFI_1	826.5	826.2	1437.4	1594.0	1.109	12.0	13.3	1.109	60.3	69.1	1.147	69	62.2
HGI_1	824.5	832.2	1355.3	1536.4	1.134	11.3	12.8	1.133	61.4	68.2	1.110	73	65.0
HEI_2	1007.1	1005.0	1678.5	1864.0	1.111	14.0	15.5	1.107	64.8	68.9	1.063	72	64.7
HFI_2	995.4	1004.0	1571.7	1668.7	1.062	13.1	13.9	1.062	61.9	71.4	1.154	76	72.2
HGI_2	994.4	1007.0	1529.8	1650.8	1.079	12.8	13.8	1.079	62.5	68.1	1.089	78	73.2
DEI_1	831.0	828.1	2374.2	2400.3	1.011	19.8	20.0	1.010	62.3	71.6	1.149	42	41.4
DFI_1	833.2	829.0	2221.7	2318.9	1.044	18.5	19.3	1.043	62.4	71.1	1.140	45	42.9
DGI_1	822.0	823.4	1934.1	2176.4	1.125	16.1	18.1	1.125	63.2	70.5	1.116	51	45.4
DEI_2	984.7	1014.1	2317.0	2622.4	1.132	19.3	21.9	1.132	66.1	75.6	1.144	51	46.4
DFI_2	1004.8	1016.0	2232.8	2290.4	1.030	18.6	19.1	1.030	68.1	74.3	1.090	54	53.2
DGI_2	984.6	1005.2	1875.5	1954.6	1.042	15.6	16.3	1.045	62.8	71.3	1.136	63	61.7
DEI_3	1029.8	1027.3	2168.1	2325.3	1.073	18.1	19.4	1.072	62.0	79.3	1.279	57	53.0
DFI_3	1026.6	1033.0	2087.9	2144.6	1.027	17.4	17.9	1.026	71.4	78.4	1.097	59	57.8
DGI_3	1020.6	1024.0	1774.9	1870.3	1.054	14.8	15.6	1.054	70.3	77.3	1.100	69	65.7

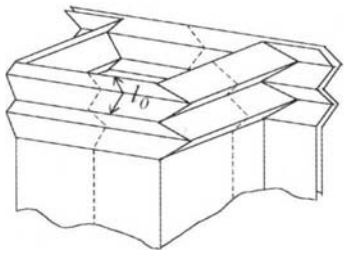

(a) Collapse mode of hat shaped section member

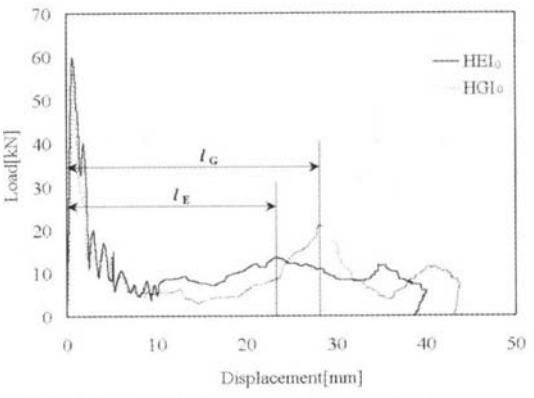

(b) Relationship between load and displacement

Fig. 9 The first folding lengths of HEI_0 and HGI_0

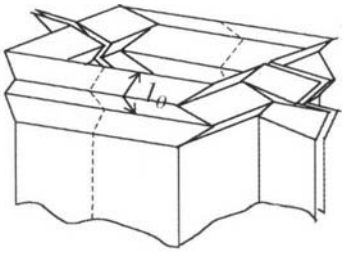

(a) Collapse mode of double hat shaped section member

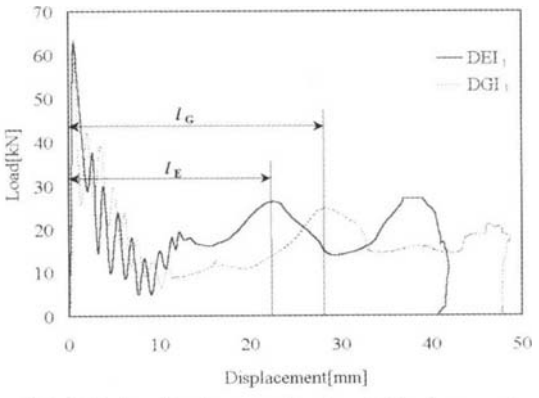

(b) Relationship between load and displacement

Fig. 10 The first folding lengths of DEI_1 and DGI_1

In Figs. 11 and 12, the decrease ratio of mean collapse load upon increasing welded pitch in the double hat shaped section members appears higher than that in the hat shaped section members. The collapse characteristics of the hat and double hat shaped section members are affected by the size of welded pitch, but the hat shaped section members are not affected greatly by the size of welded pitch because the welding line is some distance away from the center-line of the collapse load. In the double hat shaped section members, the strength between the section member of open square channel and that of flange increase significantly with the welded pitch because the welding line is at the action point of

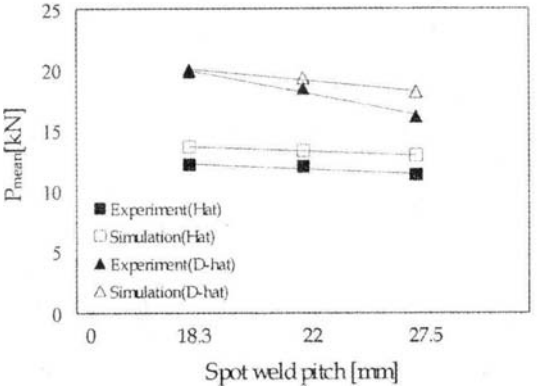

Fig. 11 Relationship between spot weld pitches and mean collapse load at a velocity of 6.54 m/sec

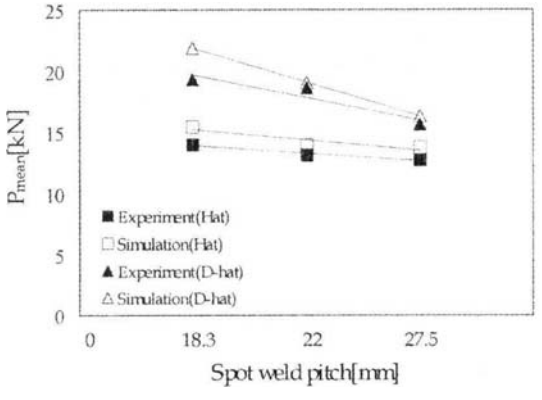

Fig. 12 Relationship between spot weld pitches and mean collapse load at a velocity of 7.19 m/sec

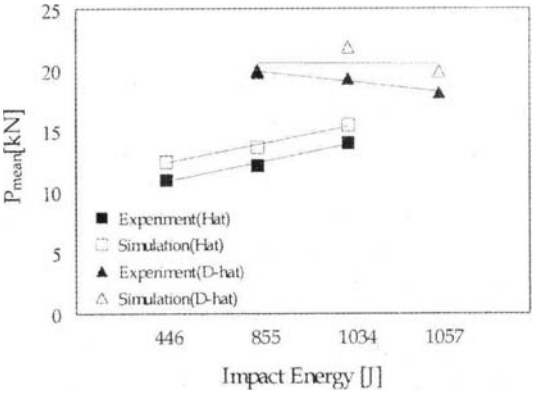

Fig. 13 Relationship between impact energy and mean collapse load at a spot weld pitch of 18.3 mm

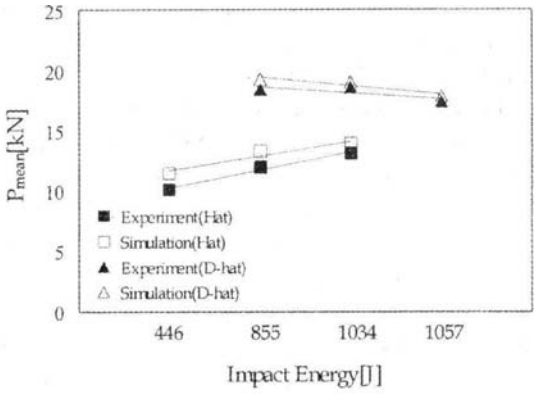

Fig. 14 Relationship between Impact energy and mean collapse load at a spot weld pitch of 22.0 mm

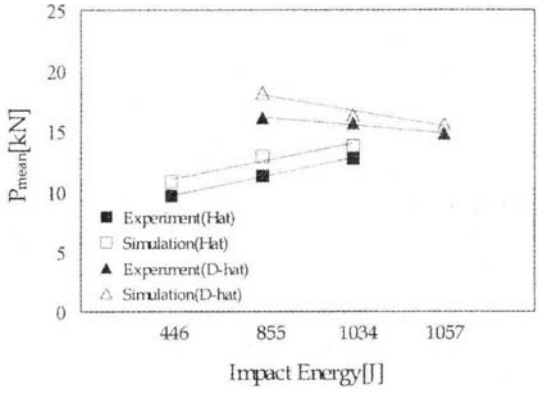

Fig. 15 Relationship between impact energy and mean collapse load at a spot weld pitch of 27.5 mm

the collapse loads. For this reason, while the hat shaped section members are easy to collapse sequentially, the double hat shaped section members are difficult to be expected to do in the sequential collapse mode. Therefore, because these effects in the double hat shaped section members are greater than those in the hat shaped section members, the larger the welded pitch is, the larger the decrease ratio of the mean collapse load is.

Table 3 and Figs. 13, 14 and 15 show the relationship between velocity change and mean collapse load at the respective spot welded pitches. In the case of the hat shaped section members, the mean collapse load increases as the velocity increases. But, in the case of the double hat shaped section members, the mean collapse load decreases as the velocity increases. The reason is as follows, and is similar to the explanation of the collapse characteristics with respect to welded pitch, the welded line in the hat shaped section members is some distance away from the center-line of the collapse load, and that in the double hat shaped section members is at the action point of the collapse loads. In the hat shaped section members, if the velocity increases, the kinetic energy increases and the sequential collapse is as expected. On the first impact, the first damage to the hat shaped section members is less than that to the double hat shaped section members, because the number of corners in the hat shaped section members is half of those in the double hat shaped section members. Therefore, in the case of hat shaped section members, the characteristics of spot welded section members do not influence the simulation greatly, because the sequential collapse mode occurs under impact collapse at a certain velocity, as the perfectly closed section members do. But, in the case of the double hat shaped section members, as the velocity increases the mean collapse load decreases, because it cannot be expected to collapse sequentially as shown in the hat shaped section members and the limit of spot welded section members appears at lower impact collapse velocities. This result shows that increased strength is important during impact collapse, but the inducement of sequential collapse is more important than that.

Also, the maximum collapse load did not appear to depend upon changing flange welded pitch, but in the hat and double hat shaped section members, the higher the impact collapse velocity is, the higher the maximum collapse load is. The tendency shown by experiment and simulation are similar, and the result of simulation appears higher than that of experiment.

On examining the results of the collapse characteristics with respect to welded pitch and the impact collapse velocity in the hat and double hat shaped section members, the total absorbed energy and mean collapse load in the double hat shaped section members are about 51% higher and the maximum collapse load is about 4.7% higher than those in the hat shaped section members under the impact collapse velocity of 6.54 m/sec. Also, the total absorbed energy and mean collapse load in the double hat shaped section members appear about 39% higher and the maximum collapse load is about 6.5% higher than those in the hat shaped section members under the impact velocity of 7.19 m/sec. If the results of experiment are compared with those of simulation, the result of simulation in the total absorbed energy and mean collapse load appeared higher by about 11.7% and the maximum collapse load appeared higher by about 11.3% than that determined by experiment in the hat shaped section members. Also, in the case of the double hat shaped section members, the results of the simulation for total absorbed energy and mean collapse load appeared higher by about 6.7%, and the maximum collapse load appeared higher by about 12.7% than determined by experiment.

5. Conclusions

In order to analyze the variation of flange welded pitch under impact collapse and the collapse characteristics under changing impact collapse velocities in spot welded hat and double hat shaped section members, both of the impact collapse experiments and impact collapse simulation by FEM was carried out. In this study, the

followings are concluded.

(1) The total absorbed energy and mean collapse loads of the hat and double hat shaped section members are lower at larger flange weld pitches. Moreover, the double hat shaped section members are more affected by weld pitch. But, the tendency of maximum collapse loads could not be found according to variations in the size of the flange weld pitch.

(2) In the hat shaped section members, the total absorbed energy and mean collapse loads increased as long as the impact collapse velocity increased, but in the double hat shaped section members, the total absorbed energy and the mean collapse load decreased. This shows that the strength is important, but it is more important to induce a sequential collapse mode under impact collapse. The maximum collapse loads appeared higher at higher impact collapse velocities in hat and double hat shaped section members.

(3) The total absorbed energy and mean collapse loads in the double hat shaped section members were about 51% higher than those of the hat shaped section members, and the maximum collapse load in the double hat shaped section members was about 4.4% higher than that of the hat shaped section members at an impact collapse velocity of 6.54 m/sec. Under an impact collapse velocity of 7.19 m/sec, the total absorbed energy and mean collapse loads in the double hat were about 39% higher than those of hat shaped section members, and the maximum collapse load in the double hat shaped section members was about 6.5% higher than that of hat shaped section members.

(4) On comparing experimental and simulation results, in the hat shaped section member, the total absorbed energy and mean collapse load by simulation were higher by about 11.7% than by experiment, and the maximum collapse load by simulation was higher by about 11.3% than the experimental result. In the double hat shaped section member, the total absorbed energy and mean collapse load in the simulation result were about 6.7% higher than those obtained by experiment, and the maximum collapse load in the simulation was about 12.7% higher than that obtained by experiment.

References

Avalle, M. and Belingardi, G., 1997, "Experimental Evaluation of the Strain Field History During Plastic Progressive Folding of Aluminium Circular Tubes," *International Journal of Mechanical Science*, Vol. 39, No. 5, pp. 575~583.

Cha, C. S., Kang, J. Y. and Yang, I. Y., 2001, "Axial Impact Collapse Analysis of Spot Welede Hat Shaped Section Members," *KSME International Journal*, Vol. 15, No. 2, pp. 180~191.

Grzebieta, R. H. and Murray, N. W., 1986, "Energy Absorption of an Initially Imperfect Strut Subjected to an Impact Load," *International Journal of Impact Engineering*, Vol. 4, pp. 147~159.

Hanssen, A. G., Langseth, M. and Hopperstad, O. S., 1999, "Static Crushing of Square Aluminium Extrusions with Aluminium Foam Filler," *International Journal of Mechanical Science*, Vol. 41, pp. 967~993.

Haug, E., Clinckemaillie, J., Ni, X., Pickett, A. K. and Queckborner, T., 1996, "Recent Trends and Advances in Crash Simulation and Design of Vehicles," *Proceedings of the NATO-ASI*, July, pp. 343~359.

John Fenton, 1996, "Handbook of Vehicle Design Analysis," *Society of Automotive Engineers*, Inc., pp. 9~12.

Jonse, N., 1989, "Structural Impact," *Cambridge University Press*, pp. 403~405.

Livermore Software Technology Corporation, 1993, *LS-DYNA3D theoretical manual*, pp. 6.1~6.10.

Livermore Software Technology Corporation, 1997, *LS-DYNA User's manual*.

Singace, A. A., 1999, "Axial Crushing Analysis of Tubes Deforming in the Multi-Lobe Mode," *International Journal of Mechanical Science*, Vol. 41, pp. 865~890.

White, M. D. and Jones, N., 1999(a), "Experimental Quasi-Static Axial Crushing of Top-Hat and Double-Hat Thin-Walled Sections," *International Journal of Mechanical Science*, Vol. 41, pp. 179~208.

White, M. D., Jones, N. and Abramowicz, W., 1999(b), "A Theoretical Analysis for the Quasi-Static Axial Crushing of Top-Hat and Double-Hat Thin-Walled Sections," *International Journal of Mechanical Sciences*, Vol. 41, pp. 209~233.